Monthly Characterization of the Tropospheric Circulation over the Euro-Atlantic Area in Relation with the Timing of Stratospheric Final Warmings

BLANCA AYARZAGÜENA AND ENCARNA SERRANO

Departamento Geofísica y Meteorología, Facultad CC. Físicas, Universidad Complutense de Madrid, Madrid, Spain

(Manuscript received 3 November 2008, in final form 1 June 2009)

ABSTRACT

In recent decades, there has been a growing interest in the study of a possible active role of the stratosphere on the tropospheric climate. However, most studies have focused on this connection in wintertime. This paper deals with the possible relationship between variations in the timing of stratospheric final warmings (SFWs, observed in springtime) and monthly averaged changes in the Euro-Atlantic climate. On the basis of the date on which the SFW occurs, two sets of years have been selected for the period of study (1958–2002): ''early years'' and ''late years,'' reflecting a very early or a very late breakup of the polar vortex. The statistical significance of the early-minus-late differences in the analyzed fields has been established by applying a nonparametric test based on a Monte Carlo–like technique. Using data from 40-yr European Centre for Medium-Range Weather Forecasts Re-Analysis (ERA-40), a dynamical study for March and April has shown important differences between both sets of years in stationary waves, especially ultralong ones (waves with $k = 1$ in March and $k = 2$ in April). Furthermore, the interannual variations in the stratospheric zonal wind seem to propagate downward as the spring progresses, in such a way that they reach tropospheric levels in April. Relevant differences between ''early'' and ''late'' years have been found in tropospheric monthly fields in the Euro-Atlantic area (geopotential, zonal wind, and storm-track activity), being at their most extensive in April.

1. Introduction

Stratospheric final warming (SFW) is one of the most important processes in the springtime stratosphere. It consists of a rapid increase in the stratospheric polar temperature, which causes the breakup of the polar vortex, which in turn involves the final transition of zonal winds from wintertime westerlies to summertime easterlies at high-latitude stratosphere (Andrews et al. 1987). This phenomenon takes place every spring in both hemispheres.

Certain studies have already shown some features of this phenomenon in the Northern Hemisphere. For instance, Black and McDaniel (2007) have analyzed the dynamic processes that take place surrounding the time of the SFW event, such as anomalous wave activity propagation and decelerations in both stratospheric and tropospheric circulations related to it. Another known and important characteristic of SFW is the large interannual variability in its timing (e.g., Waugh and Rong 2002), which some authors have already shown to be strongly dependent on planetary wave activity in the previous winter (Waugh et al. 1999; Salby and Callaghan 2007). Moreover, associated with this variability are changes that occur in other quantities—such as the stratospheric circulation and mixing processes of trace gases (Waugh and Rong 2002)—or in the polar stratospheric ozone content (Shindell et al. 1998).

In recent decades, some studies have shown evidence of a stratospheric influence on surface climate, most frequently linked to variations of the polar vortex in winter (e.g., Quiroz 1977; Baldwin and Dunkerton 1999). Recently, only a few studies have extended this analysis to spring months. Black et al. (2006) have looked at the effects of SFW events on the boreal extratropical tropospheric circulation a few days before and after this phenomenon. Other authors have associated anomalous polar stratosphere temperature in March with changes in Iberian Peninsula rainfall (López-Bustins 2006) or

Corresponding author address: Blanca Ayarzagüena, Dpto. Geofísica y Meteorología, Facultad de CC. Físicas, Universidad Complutense de Madrid, Avda. Complutense s/n, Madrid 28040 Spain.
E-mail: blanca.ayarzaguena@fis.ucm.es

DOI: 10.1175/2009JCLI2913.1

in tropospheric temperatures in the western Arctic (Overland et al. 2002). More recently, Gimeno et al. (2007) have linked the interannual variability in the timing of SFW events with variability in the number of cutoff low systems in the Northern Hemisphere in May and summer. Furthermore, Wei et al. (2007) have found a relationship between the interannual variability in the timing of SFW and variability in the lower tropospheric circulation of the Northern Hemisphere, by analyzing the 1000-hPa geopotential and 850-hPa temperature fields in February and March. However, there are still many aspects to investigate concerning the relationship between the timing of SFW and variations in tropospheric fields in spring months (until May).

The aim of the present study is to analyze a possible connection between the variations in the timing of SFWs and monthly averaged changes in the tropospheric circulation in each spring month [March–May (MAM)], especially in the Euro-Atlantic area. As far as we are aware, this work differs from previous studies in three respects. First, our analysis has been done based on monthly data in contrast to most of the studies about SFW, which are focused on daily fields surrounding the date of these events. Results from this monthly analysis could be helpful when analyzing the spring climate variability in which monthly data are usually used. Second, we examine the middle troposphere of the three spring months, in contrast to previous monthly based studies, which are focused only on the lower troposphere and also on late winter (until March). Third, as a descriptor of the tropospheric conditions, we explore the storm-track activity apart from geopotential and zonal wind fields. It should be said that the former variable has been scarcely analyzed up to now in the SFW literature and additionally, it gives us helpful information related to the regions of the strongest baroclinic wave activity, which is known to influence regional weather, especially precipitation and winds (Pinto et al. 2007).

The structure of the paper is as follows: Section 2 describes the data and methodology used in the study. In section 3, we present the main results divided in two parts: the first part describes, as a preliminary step, the differences in upward propagation of wave activity associated with the interannual variability of the SFW; and the second part—the most important part—focuses on the stratospheric–tropospheric connection related to this variability by analyzing the differences in the middle-tropospheric circulation in each spring month between years with a very early or very late breakup of the polar vortex. Lastly, section 4 presents the main conclusions.

2. Data and method

a. Database

The atmospheric data used in this study have been taken from the 40-yr European Centre for Medium-Range Weather Forecasts Re-Analysis (ERA-40; Uppala et al. 2005), with a horizontal resolution of 2.5° latitude by 2.5° longitude covering the Northern Hemisphere for the period of 1958–2002.

b. Identification of stratospheric final warming occurrence

Daily data of zonal wind at 50 hPa (U50) in 70°N from 1 March to 31 August were used to identify the dates of stratospheric final warming occurrence, according to the criterion of Black et al. (2006). These authors defined the SFW date as the final day on which the running 5-day average of the zonal mean of U50 at 70°N becomes negative and does not return to a value higher than 5 m s^{-1} until the subsequent late August. The choice of this latitude (70°N) is the result of the usual location of the polar vortex core at 50 hPa.

The large interannual variability in the timing of SFWs was noticeable once their dates were identified from the above criterion. As a result, two groups of years were selected: years when the SFW event took place very early—to be precise, more than one standard deviation (21 days) before the mean date (17 April) [hereafter ''early years'' (E); 10 cases], and years when the polar vortex broke up very late—that is, more than one standard deviation after the mean date (hereafter ''late years'' (L); 7 cases; Table 1).

c. Diagnostic tools used in the study

The core of the study consists of a month-by-month analysis (MAM) of the differences between both sets of years (early and late) in different fields at the middle troposphere and through the whole atmospheric column (23 pressure levels up to 1 hPa). This has been carried out by creating composite maps of monthly variables and then applying a nonparametric test, based on a Monte Carlo–like technique (described later) to establish, for each spring month, the statistical significance of the differences between years when the polar vortex is very persistent (late years) and years when it disappears very soon (early years). As mentioned earlier, the study carried out is composed of the two following parts.

1) DYNAMICAL STUDY

A study of the relationship between the timing of the SFW and variations in eddy flux and in eddy forcing of the mean flow in the 3-month sequence (MAM) is

TABLE 1. Dates of occurrence of the stratospheric final warming events in the period of 1958–2002 according to the criterion of Black et al. (2006).

Day	Year	Day	Year
1 May	1958	22 May	1981 (L)
2 April	1959	23 April	1982
22 April	1960	21 March	1983 (E)
19 March	1961 (E)	13 March	1984 (E)
6 May	1962	4 April	1985
9 April	1963	29 April	1986
24 March	1964 (E)	8 May	1987 (L)
22 April	1965	19 April	1988
6 April	1966	15 April	1989
9 May	1967 (L)	3 June	1990 (L)
2 May	1968	5 May	1991
14 April	1969	12 April	1992
12 April	1970	14 April	1993
16 March	1971 (E)	3 April	1994
27 March	1972 (E)	26 April	1995
26 May	1973 (L)	8 April	1996
26 March	1974 (E)	3 May	1997
20 March	1975 (E)	26 March	1998 (E)
18 April	1976	6 May	1999
12 April	1977	24 April	2000
27 March	1978 (E)	4 June	2001 (L)
4 April	1979	10 May	2002 (L)
7 April	1980		

performed. This study is performed using the transformed Eulerian mean (TEM) formulation in the quasigeostrophic approximation—in particular, the transformed mean zonal momentum equation in a beta-plane geometry with pressure as the vertical coordinate (Edmon et al. 1980):

$$\frac{\partial \overline{u}}{\partial t} - f\overline{v}^* - \overline{\Im} = \overline{\mathbf{V}} \cdot \hat{\mathbf{F}}, \tag{1}$$

where overbars indicate zonal mean, u is the zonal wind, f is the Coriolis parameter, $\overline{v}^*$ is the meridional component of the residual meridional circulation, $\overline{\Im}$ is the Eulerian-mean friction, and $\hat{\mathbf{F}}$ is the Eliassen–Palm flux (hereafter EP flux). The meridional component of the residual meridional circulation is defined as

$$\overline{v}^* = \overline{v} - \frac{\partial\left[\overline{v'\theta'}\left(\frac{\partial\overline{\theta}}{\partial p}\right)^{-1}\right]}{\partial p}, \tag{2}$$

where primes indicate departures from the zonal mean, θ is the potential temperature, and p is the pressure.

The EP flux is defined as

$$\hat{\mathbf{F}} = \left[0,\ -\overline{v'u'},\ f\overline{v'\theta'}\left(\frac{\partial\overline{\theta}}{\partial p}\right)^{-1}\right]. \tag{3}$$

As shown by Edmon et al. (1980), the $\hat{\mathbf{F}}$ constitutes a measure of the Rossby wave propagation from one height (p) and latitude (ϕ) to another. Furthermore, its divergence (divEP) gives us information about the forcing of the mean flow by the eddies.

In this work we have computed cross sections of monthly anomalies of EP flux and its divergence for the total stationary waves and also for different zonal wavenumbers (using fast Fourier transform filters). In these representations, we have adopted the conventions indicated by Edmon et al. (1980) to obtain an appropriate representation in a (ϕ–log$p$) plane. Therefore, the EP flux and divergence represented in the vertical diagrams are as follows:

$$\mathbf{F} = (F_\phi,\ F_p) = 2\pi r_0^2 g^{-1}\cos\varphi \times\left[-p\,\overline{v'u'},\ fr_0\overline{v'\theta'}\left(\frac{\partial\overline{\theta}}{\partial p}\right)^{-1}\right] \quad \text{and} \tag{4}$$

$$\text{divEP} = \frac{\partial}{\partial\varphi}(F_\phi) + \frac{\partial}{\partial(\log p)}(F_p), \tag{5}$$

where g is the gravitational acceleration and r_0 is the radius of the earth.

Furthermore, because the two axes of the diagrams have different scales, the horizontal and vertical arrow components of $\mathbf{F}$ as measured in the diagram have been calculated by multiplying their values by the distances occupied by 1 "unit" in the corresponding axis on the diagram [i.e., F_ϕ by a radian of latitude and F_p by 1 (because the vertical axis does not have units)].

2) RELATION BETWEEN VARIABILITY IN THE SPRINGTIME STRATOSPHERE AND TROPOSPHERE

The possible effect of the interannual variability of the SFW on the middle-tropospheric circulation over the Euro-Atlantic area is explored by composite maps. We have analyzed the monthly anomalies of storm-track activity at 500 hPa, which was calculated by the standard deviation of the bandpass (2–6 days) filtered variability of geopotential at such level (Ulbrich et al. 2008). Also, we extended this analysis to geopotential and zonal wind at 500 hPa.

d. Statistical significance of results

It is well known that when evaluating the statistical significance of data fields defined over large spatial networks for small samples, the normality and independence of the data values cannot safely be assumed. Thus, the use of classical tests to make significance

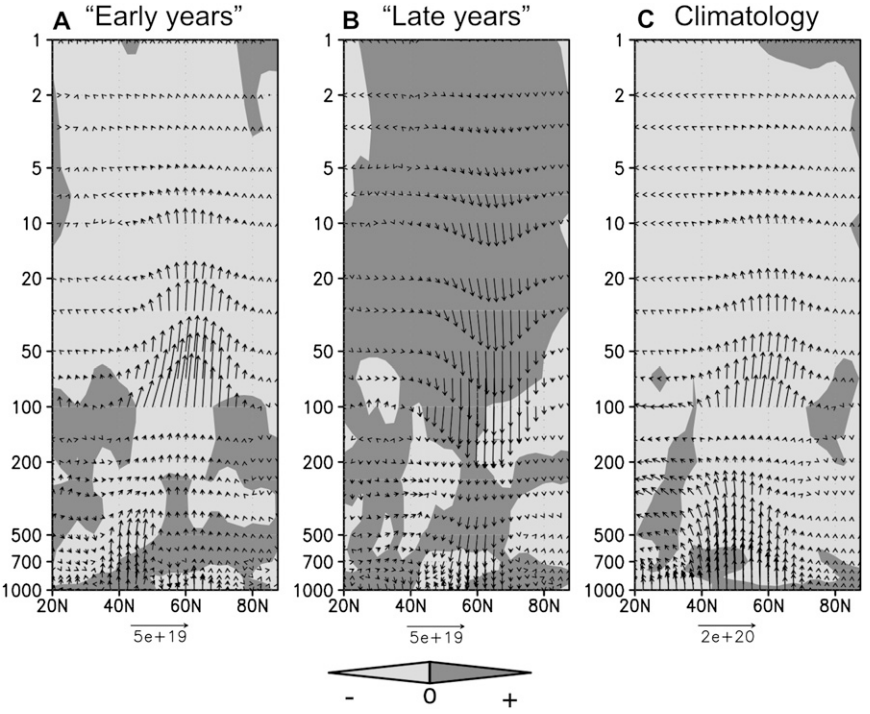

FIG. 1. Composites of anomalous EP flux (arrows) with its divergence (shading) in March for (a) early years (10 cases) and (b) late years (7 cases). (c) Climatology of EP flux and its divergence. Arrow scale (m^3 Pa) is indicated at the bottom. Scaling arrow at 100 hPa and higher is divided by a factor of 10 so that EP flux can be appreciated more easily. (Notice that an arrow pointing downward—i.e., toward high pressures—indicates that F_p is positive). Light (dark) shading shows negative (positive) values of EP flux divergence.

statements (e.g., Student's t, Fisher–Snedecor) is not adequate (Preisendorfer and Barnett 1983). To avoid this type of problem, permutation procedures (e.g., Monte Carlo techniques) are frequently used to generate the probability density function (pdf) on which the statistical test of significance is based (Livezey and Chen 1983; Czaja and Frankignoul 1999; Rodríguez-Fonseca et al. 2006).

In the present study, we have applied an adaptation of the so-called pool permutation procedure designed by Preisendorfer and Barnett (1983) to construct the associated pdf of the statistic that measures the difference between a pair of datasets to be compared (in this study, between early and late years).

Here **E** and **L** denote the two datasets of a certain variable (i.e., monthly geopotential at 500 hPa in April)—n_E and n_L years for early years and late years, respectively—over s grid points. We can consider **E** and **L** as two sets of n_E and n_L points in a Euclidean space (ε_s) of dimension s:

$$\mathbf{E} = \{\mathbf{e}(t): \quad t = 1, 2, \ldots\ldots, n_E\} \quad \text{and} \tag{6}$$

$$\mathbf{L} = \{\mathbf{l}(t): \quad t = 1, 2, \ldots\ldots, n_L\}, \tag{7}$$

where $\mathbf{e}(t)$ and $\mathbf{l}(t)$ represent vectors of s components for the time t. Consequently, the centroids of the two sets of points, **E** and **L**, are defined by the vectors

$$\bar{\mathbf{e}} \equiv \frac{1}{n_E}\sum_{t=1}^{n_E}\mathbf{e}(t) \quad \text{and} \quad \bar{\mathbf{l}} \equiv \frac{1}{n_L}\sum_{t=1}^{n_L}\mathbf{l}(t), \tag{8}$$

whose graphical representations in geographical coordinates are the known composites maps. In this way, the measure of discrepancy for each x grid point between **E** and **L** used in this work is

$$\mathrm{DIF}(x) \equiv \left[\frac{1}{n_E}\sum_{t=1}^{n_E} e(t, x)\right] - \left[\frac{1}{n_L}\sum_{t=1}^{n_L} l(t, x)\right] \quad x = 1, \ldots, s; \tag{9}$$

that is, the difference of the corresponding time means. Overall, DIF(x) is the x component of the vector **DIF** ($= \{\mathrm{DIF}(x)\}_{x=1,\ldots,s}$), which is illustrated by an early-minus-late (hereafter E minus L) difference composite map.

The method of establishing the statistical significance of differences between early and late years is as follows.

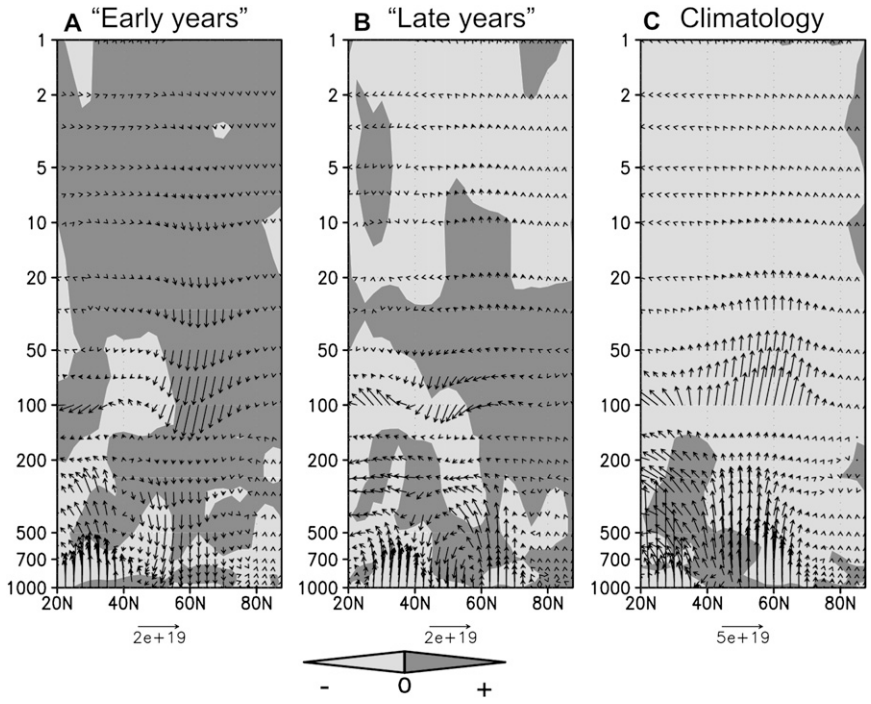

FIG. 2. Same as Fig. 1, but for April.

The first step of the generation of the pdf of the statistic DIF (for each grid point of a given atmospheric field) is the union (**U**) of the two datasets **E** and **L** in ε_s, thereby forming a single batch of $n_E + n_L$ elements. The batch **U** is then repeatedly partitioned randomly (5000 times in this work) into batches $\mathbf{U_1}$ and $\mathbf{U_2}$ with n_E and n_L elements, respectively. The statistic **DIF** vector of the pair $[\mathbf{U_1}, \mathbf{U_2}]$ is computed for each permutation of 1, 2, . . . , $n_E + n_L$. The resultant set of values of gridpoint DIF formed by all generated partitions is used to construct its pdf. Once each gridpoint DIF of the two original sets **E** and **L** (denoted by DIF*) is computed, we can determine its location in the associated pdf. From this, we can decide whether each gridpoint DIF* is large by chance or not. In other words, we can establish the statistical significance level of the DIF* for each grid point or determine whether this value is statistically significant at a given significance level (e.g., $\alpha = 0.05$, value used in this work).

3. Results

In this section we present results obtained from a comparative analysis of the circulation and dynamical properties in each spring month (MAM) between early and late years. As it was defined in section 2, the former set corresponds to years when the SFW took place between 13 and 27 March, whereas the latter set occurred between 8 May and 4 June. Following the order used in the description of the previous section, the results are discussed in two parts.

a. Dynamical study

Here, results obtained when analyzing the variations in the wave activity in each spring month related to an early or late breakup of the polar vortex are presented. We should say that this part of the study shows only March and April, because the seasonal cycle, the wave activity, and its interannual changes in May are negligible in comparison with the two previous months.

The first aspect analyzed was the interannual variability of stationary waves. As seen in Figs. 1 and 2, both March and April present noticeable differences in the EP flux, especially in the vertical component (F_p) and divergence (divEP) between the two sets of years. Moreover, some of these differences in F_p and divEP are statistically significant, particularly in March (Fig. 3). Because the F_p and divEP give us information about the vertical propagation of the wave activity and its effect on the mean flow, respectively, this result is meaningful.

In the case of early years, the results agree well with the theory on upward propagation of wave activity by Charney and Drazin (1961). In March, the polar vortex is weaker than normal (Figs. 4a and 4c) and stationary waves propagate more than average from the troposphere to the stratosphere. This is consistent with more deceleration of the mean flow than average in the stratosphere, as

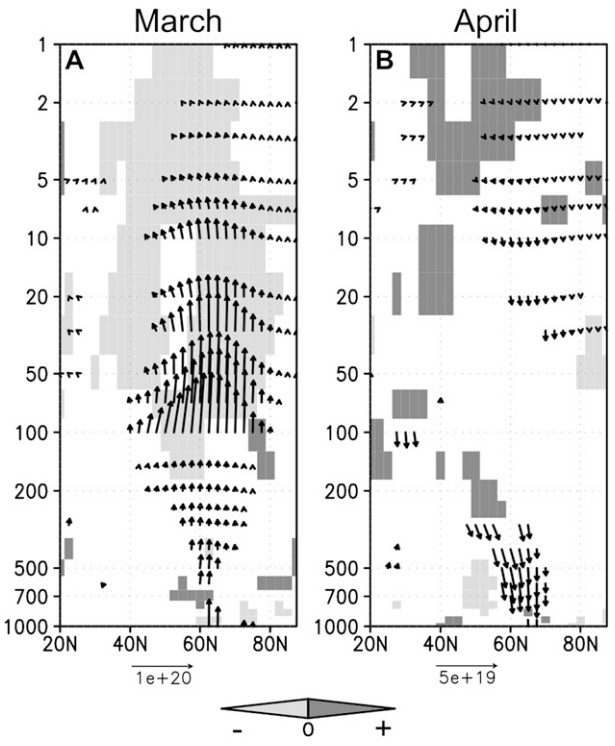

FIG. 3. E-minus-L difference composites of anomalous EP flux (arrows) with its divergence (shading) for (left) March and (right) April. Scaling arrow at 100 hPa and higher is divided by a factor of 10 so that EP flux may be easily seen. Arrows are drawn when the vertical component of the EP flux is statistically significant at a 95% confidence level. Light (dark) shadings indicate negative (positive) statistically significant differences of EP flux divergence at 95%.

expected in a weak vortex that satisfies the definition of early years (compare the anomalies of F_p and divEP in Fig. 1a with Fig. 1c). The opposite occurs in April because the polar vortex has already disappeared in early years (Fig. 5a) and thus these conditions do not facilitate wave propagation into the stratosphere (Figs. 2a and 2c).

In the case of late years, the results are consistent with Charney–Drazin's theory as well, but it is worth highlighting some aspects. In March, a large absence of wave activity is found, whereas in April the anomalies of EP flux are much less important. Thus, in March, we observe a large column of positive F_p anomalies centered on 60°N and extended up to the whole stratosphere—and a predominance of positive anomalies of divEP in the extratropical stratosphere, too (Fig. 1b; opposite sign from results for early years). In contrast, in April, we can only point out the anomalous upward propagation in the band 60°–70°N up to the upper troposphere, turning there toward the equator (Fig. 2b). These results for late years could mean that there are relevant anomalies in both tropospheric and stratospheric wave activity one to two months before the SFW event (i.e., in March), but as the time progresses (in April), the anomalous wave activity is weaker.

The contribution of each zonal wavenumber (k) disturbance to the differences in the wave upward propagation between early and late years has been also analyzed. In March, the zonal wavenumber-1 wave is the component that most explains the pattern of differences in the EP flux between early and late years (see Fig. 6a and compare with Fig. 3a and 6c). Results obtained by other authors seem to support this finding: Black and McDaniel (2007) observed anomalous upward propagation of waves with wavenumber 1 associated with SFW events (applicable to our early years), and Limpasuvan et al. (2004) showed that the main contributor to the negative anomalies of meridional eddy flux of heat related to the recovery of polar vortex after a stratospheric sudden warming (SSW) is a wave of $k = 1$. This could be comparable to our results corresponding to March for late years, because in more than half of these cases (four out of seven), a major SSW was identified in February or at the beginning of March. However, we should bear in mind that the present analysis is based on monthly averages, whereas the mentioned works are based on daily data.

In April, even though a wave of $k = 1$ plays an important role in the upper stratosphere, it is a wave of $k = 2$ that appears to explain the greatest part of the pattern of E-minus-L differences in the total EP flux, in both troposphere and stratosphere (Figs. 6b, 6d, and 3b).

The same analysis with transient waves for early and late years has been also carried out. However, the areas with statistical significant differences for these waves between these two sets of years are not as extensive as those corresponding to stationary waves, which is particularly clear in March (not shown). It should be added that the predominance of stationary waves at mid- and high latitudes has also been identified by some authors, although related to events of stratosphere–troposphere coupling in winter (Limpasuvan and Hartmann 2000; Limpasuvan et al. 2004; or Haklander et al. 2007).

b. Relation between variability in the springtime stratosphere and troposphere

Figure 7 shows the E-minus-L differences in the monthly zonal-mean zonal wind $\overline{u}$ along the atmospheric column (up to 1 hPa) in March, April, and May. In these cross sections, we can appreciate that the statistically significant negative differences (i.e., $\overline{u}$ is stronger in late than in early years) shift downward as the spring season progresses; however, in March, they are restricted to the upper and middle stratosphere, the statistically significant E-minus-L differences of $\overline{u}$ in April extend through the whole extratropical stratosphere, and even reach the surface in a very narrow high-latitude band (60°–70°N).

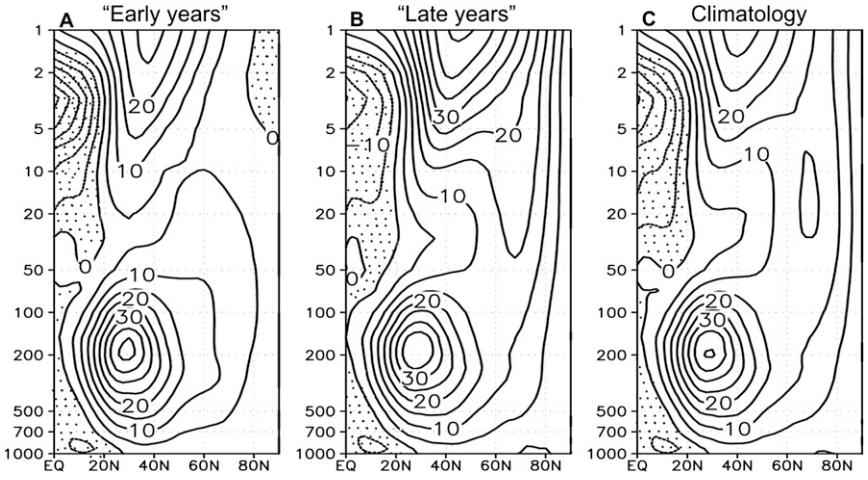

FIG. 4. Composite cross section of the zonal-mean zonal wind in March for (a) early years and (b) late years, and (c) the climatology. Contour interval is 5 m s^{-1}. Stippled regions correspond to negative values.

Although the differences of $\overline{u}$ in May are much lower than in the two previous months, we still observe statistically significant values in the stratosphere about the 60°–80°N latitude band, which extend weakly downward, reaching 500 hPa around 70°N. Also, a small center of positive differences appears at polar latitudes (80°–90°N) in the middle troposphere in May. This latter result is quite reliable, taking into account the zonal distribution of the angular momentum, despite the deficiencies in the current reanalysis data north of 80°N.

As differences in stratosphere seem to spread downward (as just mentioned), an analysis of middle tropospheric fields has been performed. We have studied the storm-track activity at 500 hPa in the 3-month MAM sequence. Because this variable informs us about areas with the strongest baroclinic wave activity and that the latter measures the synoptic activity, this analysis appears to be an adequate way of exploring the stratosphere–troposphere connection. In addition, very few studies about SFW have considered this variable up to now.

As we can see in Fig. 8, the major statistically significant E-minus-L differences in storm-track activity were found in April (at a 95% confidence level). In fact, in this month, these differences in the North Atlantic area were conspicuous. Taking this into account, and the fact that the polar vortex state in April is completely different between the two types of years, hereafter we will restrict the discussion of results to this spring month.

When comparing the storm-track activity in the months of April in early years with the climatology (Fig. 9a versus Fig. 9c), we can see a southward shift in the east coast of North America (where the Atlantic maximum

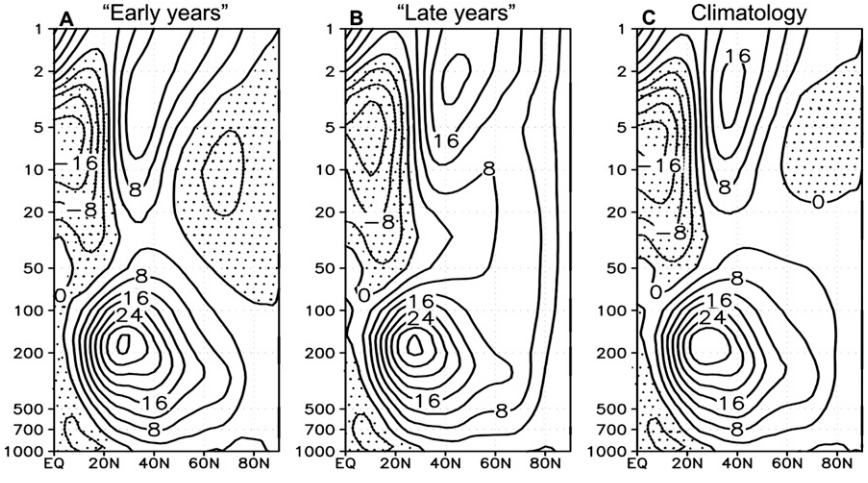

FIG. 5. Same as Fig. 4, but for April. Contour interval is 4 m s^{-1}.

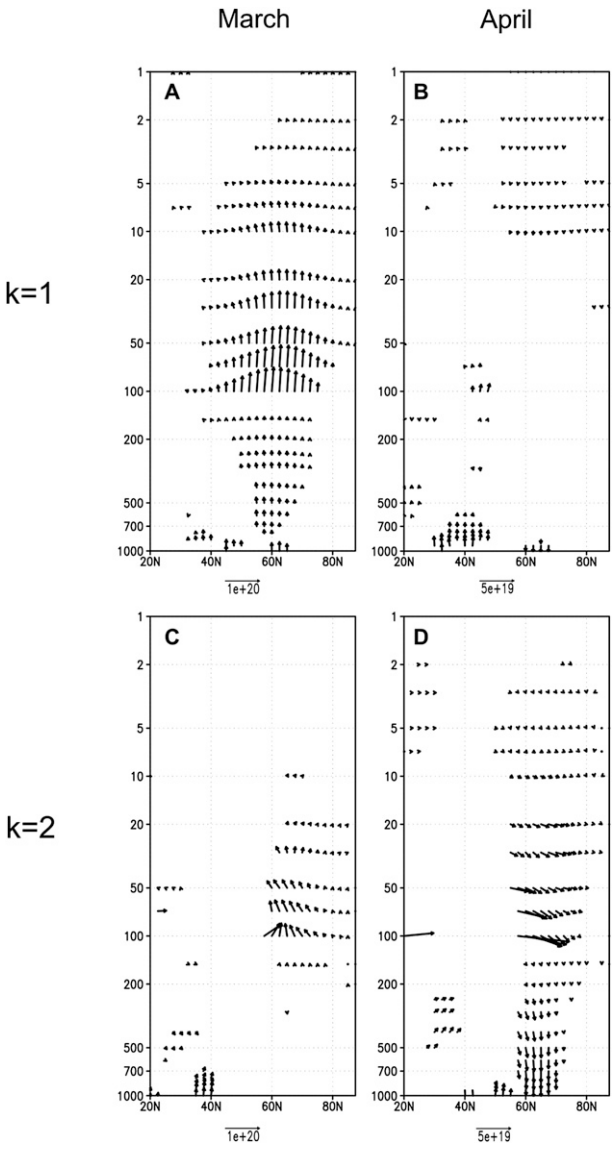

FIG. 6. E-minus-L composites of EP flux corresponding to (left) March and (right) April for the wavenumbers (a),(b) 1 and (c),(d) 2. Scaling arrow at 100 hPa and higher is divided by a factor of 10 so that EP flux can be easily seen. Arrows are drawn when the vertical component of the EP flux is statistically significant at 95%.

of this field is found) and a weakening along the whole Atlantic strip. The opposite is observed for late years (Fig. 9b): the maximum of the storm-track activity is located northward with respect to the climatology and, what is more, the values greater than 40 m cross the British Isles and reach the Scandinavian Peninsula. The importance and reliability of these discrepancies between early and late years is supported by the statistical significance of the E-minus-L composite of storm-track activity (Fig. 8b). Notice that statistically significant differences have been identified both in the entrance (North American coast) and exit (Scandinavia) regions of the storm tracks in the Atlantic area.

Moreover, when analyzing the propagation of stationary wave activity in the horizontal plane at tropospheric levels, we obtain consistent results with those of the storm tracks' activity (not shown). To be precise, the major wave train in the North Atlantic basin is shifted equatorward (poleward) with respect to the average in early (late) years, the same as what happens to storm-track activity. This would imply that the E-minus-L differences in the stationary wave propagation described in the previous subsection could be related to those found in storm-track activity. In fact, certain model simulations have already provided evidence that planetary stationary waves play an important role in the organization and maintenance of the storm tracks (Broccoli and Manabe 1992; Lee and Mak 1996; Chang et al. 2002).

We may also infer from the above results that in years when the SFW occurs late, a higher number of storms cross North Europe in April. For early years we could conclude just the opposite.

The next step of the study was to evaluate the effects of the interannual variability in the timing of SFW on the usual variables 500-hPa geopotential and zonal wind (hereafter Z500 and U500, respectively) in MAM. As in the case of storm-track activity, the differences in the composites of these two fields for the 3-month sequence MAM between early and late years are noticeable. In fact, the anomalies show, in general, opposite signs for each set of years in most of the Euro-Atlantic region (e.g., Fig. 10), but it is again in April when these differences of both variables are at their most extensive and display the highest values (particularly for U500).

In April of the late years, a tripole of Z500 anomalies is found in the North Atlantic area and is composed of negative values over high latitudes and the subtropical Atlantic, and positive anomalies off the west of the British Isles (Fig. 10b). In contrast, the atmospheric pattern in early years is quite different from that corresponding to late years: not only in the sign of the centers of action, but also because these centers are weaker, shifted, and deformed (Fig. 10a). In fact, the hemispheric pattern for late years resembles the positive phase of Arctic Oscillation (AO); however, the hemispheric pattern of the early years does not resemble the negative AO phase. Notice that the main centers of action of the composites of Fig. 10 are statistically significant (at a 95% confidence level, from a Monte Carlo test using 5000 permutations). The discrepancies between early and late years in Z500 can also be observed in the E-minus-L composite, where we can see two statistically significant centers over high and middle latitudes, and another secondary one over the subtropical Atlantic

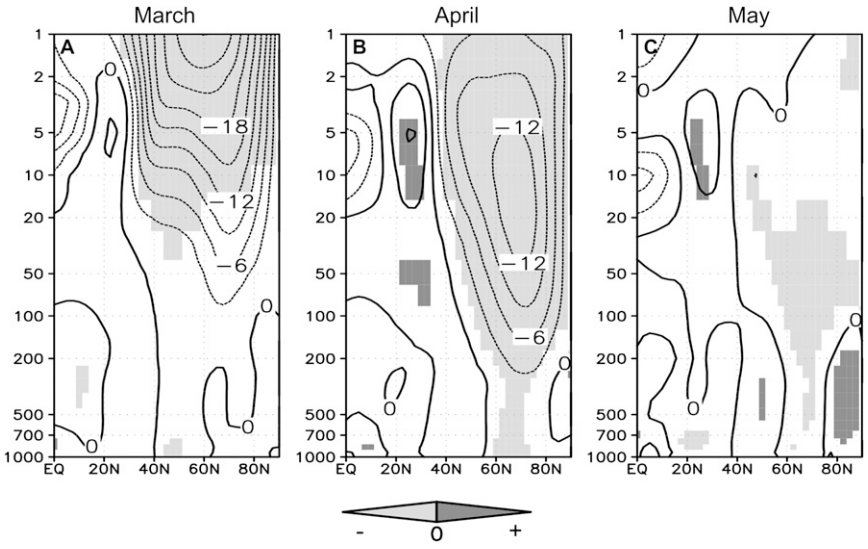

FIG. 7. E-minus-L composites of the zonal-mean zonal wind. Contour interval is 3 m s^{-1}. Light (dark) shading corresponds to negative (positive) statistically significant differences at 95%.

(Fig. 11a). This result is consistent with the corresponding E-minus-L pattern of U500 (Fig. 11b), as the antinodes are located over the regions where the gradient of the E-minus-L differences in Z500 is at a maximum. It also agrees with the pattern of storm-track activity, because the westerlies in early years (late years) seem to be weaker (stronger) than average at high latitudes in the North Atlantic basin and stronger (weaker) at midlatitudes, coincident with the southward (northward) shift of maximum in the storm-track activity.

Lastly, because the AO phase is related to the variation in the polar vortex strength, we have checked whether there is any statistical dependency between the AO phase (positive or negative) in April and the late–early occurrence of the SFW. Because the expected frequencies (if the two characters were independent) are small, we have carried out this analysis by using a Fisher–Irwin exact test, in which the null hypothesis H_0 is the ''independence between characters'' (Hodges and Lehmann 2004). Bear in mind that, in this type of tests, the lower the confidence level, the more reliable the acceptance of H_0. The result of applying the Fisher–Irwin test to our case indicates that we would accept H_0 with an ''exact'' confidence level of 92%. Looking at Table 2, we can see that late years seem to be related to the positive phase of the AO in April (because six out of seven late years were under AO^+). In contrast, early years do not project strongly onto a certain AO phase, probably because the strength of the AO decreases in nonwinter circulation regimes. In March, statistical independence was concluded between the AO phase in this month and the early–late occurrence of the SFW as well, even with an

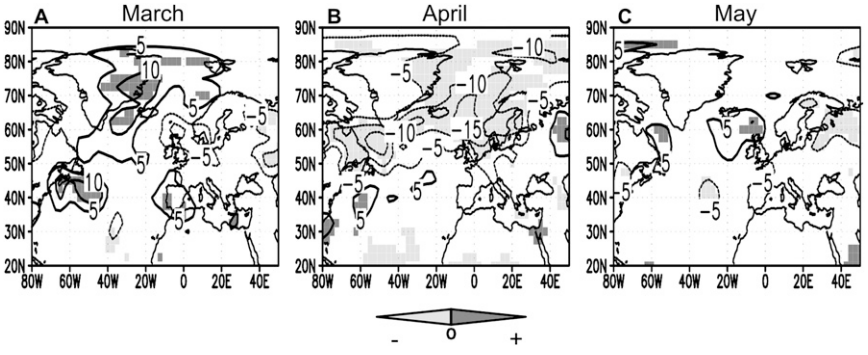

FIG. 8. E-minus-L composites of storm-track activity at 500 hPa for (a) March, (b) April, and (c) May. Contour interval is 5 gpm. Light (dark) shading indicates negative (positive) statistically significant differences at 95%. Zero contours are omitted for clarity.

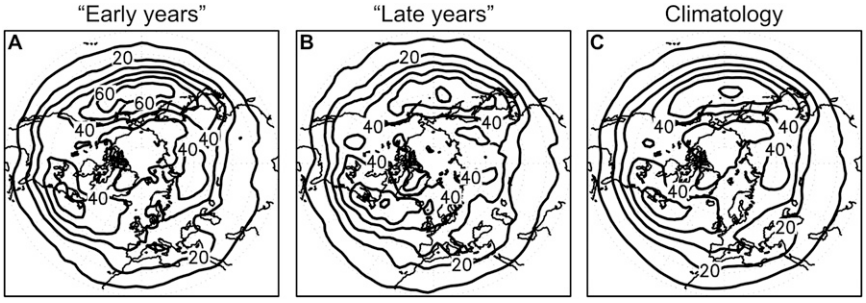

FIG. 9. Composites of storm-track activity at 500 hPa in April for the (a) early years, (b) late years, and (c) climatology. Contour interval is 10 gpm.

exact confidence level much lower than for April (i.e., 70%). Therefore, these results indicate that the present work is not a comparison of the influence of stratospheric changes on the tropospheric variability based on the AO phase; as some studies have already done, e.g., Baldwin and Dunkerton (2001).

4. Summary and conclusions

This study explores a possible relationship between the interannual variability in the timing of stratospheric final warmings (SFWs) and monthly variability in the springtime tropospheric circulation, especially in the Euro-Atlantic area. Our results show that this link exists by analyzing some aspects, such as the tropospheric wave propagation toward the stratosphere and midtropospheric storm-track activity. This analysis consists of a comparison of different monthly atmospheric patterns—for March, April and May—between two groups of years: those with nonpersistent vortex (''early years'') and those with very persistent vortex (''late years'').

The main findings can be summarized as follows:

- Regarding dynamical aspects, cross sections of monthly anomalies of EP flux and its divergence indicate relevant interannual differences in stationary waves; most of them explained by variations in ultra long ones ($k = 1$ in March and $k = 2$ in April). These differences are more important in March than in April, with opposite behavior in some areas between both months.
- The statistically significant differences between early and late years in the monthly zonal-mean zonal wind seem to propagate downward from the upper stratosphere as the spring season progresses, in such a way that in April these differences reach the lowermost stratosphere and even the troposphere in 60°–70°N.
- The late or early occurrence of the yearly SFW seems to have some effect on the troposphere over the Euro-Atlantic area, especially in April.

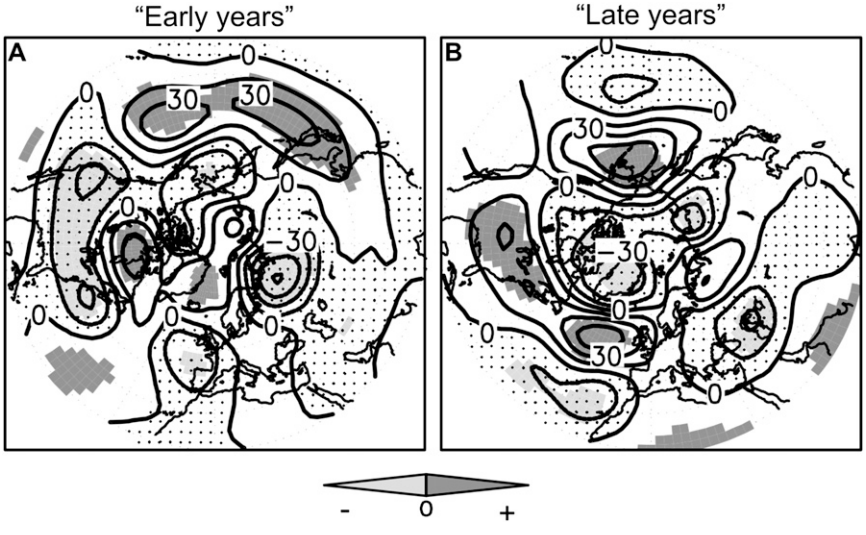

FIG. 10. Composites of Z500 anomalies in April for (a) early and (b) late years. Contour interval is 15 gpm. Stippled regions correspond to negative values and shaded areas to statistically significant values at 95%.

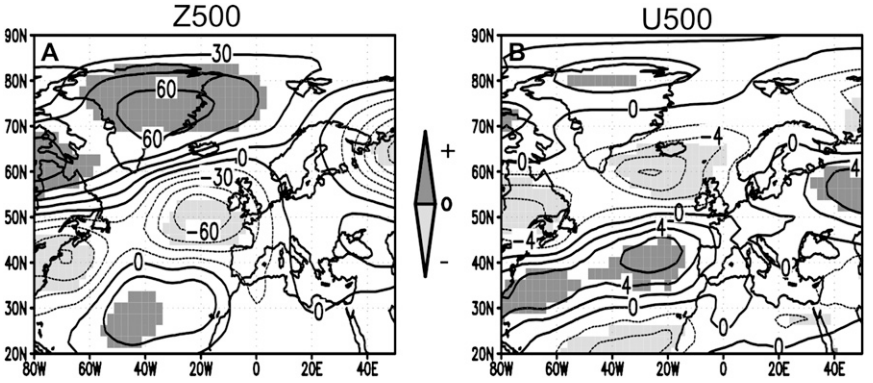

FIG. 11. E-minus-L composites of (a) geopotential (contour interval: 15 gpm) and (b) zonal wind (contour interval: 2 m s^{-1}) at 500 hPa in April. Light (dark) shading corresponds to negative (positive) statistically significant values at 95%.

- Statistically significant differences between early and late years are identified in the entrance and exit regions of the storm tracks over the North Atlantic sector. Late years (early years) are characterized by a northward (southward) shift of the storm tracks, which would lead to a higher (lower) number of storms crossing North Europe in April. This type of analysis is new in the SFW literature.
- Concerning the 500-hPa zonal wind, the westerlies appear weaker (stronger) than mean values at high latitudes in the North Atlantic basin and stronger (weaker) at middle latitudes in early (late) years. Consistent results are found for the 500-hPa geopotential anomalies.
- Results from a Fisher–Irwin exact test support the hypothesis that the type of years (early or late) is independent of the Arctic Oscillation phase, even though the geopotential pattern in mid-springtime in late years resembles the positive AO phase. This implies a new contribution with respect to previous studies based on the differences in the tropospheric circulation between AO phases.

Acknowledgments. This study was funded by the Spanish MEC Projects CGL2005-06600-C02 and CGL2008-06295, the European Social Fund, and the ''Consejería de Educación de la Comunidad de Madrid.'' The ERA-40 data are available online (at http://data.ecmwf.int/data/index.html). The authors thank Prof. C. R. Mechoso, Prof. P. Zurita, and the anonymous reviewers for their helpful suggestions and comments.

TABLE 2. Contingency table displaying the number of early years and late years (in the period 1958–2002) with positive or negative AO phase in April.

	AO positive	AO negative	Total
Early years	4	6	10
Late years	6	1	7
Total	10	7	17

REFERENCES

Andrews, D. G., J. R. Holton, and C. B. Leovy, 1987: *Middle Atmosphere Dynamics*. Academic Press, 489 pp.

Baldwin, M. P., and T. J. Dunkerton, 1999: Propagation of the Arctic Oscillation from the stratosphere to the troposphere. *J. Geophys. Res.,* **104,** 30 937–30 946.

——, and ——, 2001: Stratospheric harbingers of anomalous weather regimes. *Science,* **294,** 581–584.

Black, R. X., and B. A. McDaniel, 2007: The dynamics of Northern Hemisphere stratospheric final warming events. *J. Atmos. Sci.,* **64,** 2932–2946.

——, ——, and W. A. Robinson, 2006: Stratosphere–troposphere coupling during spring onset. *J. Climate,* **19,** 4891–4901.

Broccoli, A. J., and S. Manabe, 1992: The effects of orography on midlatitude Northern Hemisphere dry climates. *J. Climate,* **5,** 1181–1201.

Chang, E. K. M., S. Lee, and K. L. Swanson, 2002: Storm track dynamics. *J. Climate,* **15,** 2163–2183.

Charney, J. G., and P. G. Drazin, 1961: Propagation of planetary-scale disturbances from the lower into the upper atmosphere. *J. Geophys. Res.,* **66,** 83–109.

Czaja, A., and C. Frankignoul, 1999: Influence of the North Atlantic SST on the atmospheric circulation. *Geophys. Res. Lett.,* **26,** 2969–2972.

Edmon, H. J., B. J. Hoskins, and M. E. McIntyre, 1980: Eliassen–Palm cross sections for the troposphere. *J. Atmos. Sci.,* **37,** 2600–2616.

Gimeno, L., R. Nieto, and R. M. Trigo, 2007: Decay of the Northern Hemisphere stratospheric polar vortex and the occurrence of cut-off low systems: An exploratory study. *Meteor. Atmos. Phys.,* **96,** 21–28.

Haklander, A. J., P. C. Siegmund, and H. M. Kelder, 2007: Interannual variability of the stratospheric wave driving during northern winter. *Atmos. Chem. Phys.,* **7,** 2575–2584.

Hodges, J. L., Jr., and E. L. Lehmann, 2004: *Basic Concepts of Probability and Statistics*. 2nd ed. Society for Industrial and Applied Mathematics, 441 pp.

Lee, W.-J., and M. Mak, 1996: The role of orography in the dynamics of storm tracks. *J. Atmos. Sci.,* **53,** 1737–1750.

Limpasuvan, V., and D. L. Hartmann, 2000: Wave-maintained annular modes of climate variability. *J. Climate,* **13,** 4414–4429.

——, D. W. J. Thompson, and D. L. Hartmann, 2004: The life cycle of the Northern Hemisphere sudden stratospheric warmings. *J. Climate,* **17,** 2584–2596.

Livezey, R. E., and W. Y. Chen, 1983: Statistical field significance and its determination by Monte Carlo techniques. *Mon. Wea. Rev.,* **111,** 46–59.

López-Bustins, J. A., 2006: Temperatura de la estratosfera polar y precipitación de la Península Ibérica en marzo (1958-2000). *Clima, Sociedad y Medio Ambiente,* J. M. Cuadrat Prats, Eds., Serie A, Vol. 5, Publicaciones de la Asociación Española de Climatología, 175–189.

Overland, J. E., M. Wang, and N. A. Bond, 2002: Recent temperature changes in the western arctic during spring. *J. Climate,* **15,** 1702–1716.

Pinto, J. G., U. Ulbrich, G. C. Leckebusch, T. Spangehl, M. Reyers, and S. Zacharias, 2007: Changes in storm track and cyclone activity in three SRES ensemble experiments with the ECHAM5/MPI-OM1 GCM. *Climate Dyn.,* **29,** 195–210.

Preisendorfer, R. W., and T. P. Barnett, 1983: Numerical model–reality intercomparison tests using small-sample statistics. *J. Atmos. Sci.,* **40,** 1884–1896.

Quiroz, R. S., 1977: The tropospheric-stratospheric polar vortex breakdown of January 1977. *Geophys. Res. Lett.,* **4,** 151–154.

Rodríguez-Fonseca, B., I. Polo, E. Serrano, and M. Castro, 2006: Evaluation of the North Atlantic SST forcing on the European and Northern African winter climate. *Int. J. Climatol.,* **26,** 179–191.

Salby, M. L., and P. F. Callaghan, 2007: Influence of planetary wave activity on the stratospheric final warming and spring ozone. *J. Geophys. Res.,* **112,** D20111, doi:10.1029/2006JD007536.

Shindell, D., D. Rind, and P. Lonergan, 1998: Increased polar stratospheric ozone losses and delayed eventual recovery owing to increasing greenhouse-gas concentrations. *Nature,* **392,** 589–592.

Ulbrich, U., J. G. Pinto, H. Kupfer, G. C. Leckebusch, T. Spangehl, and M. Reyers, 2008: Changing Northern Hemisphere storm tracks in an ensemble of IPCC climate change simulations. *J. Climate,* **21,** 1669–1679.

Uppala, S. M., and Coauthors, 2005: The ERA-40 Re-Analysis. *Quart. J. Roy. Meteor. Soc.,* **131,** 2961–3012.

Waugh, D. W., and P. P. Rong, 2002: Interannual variability in the decay of lower stratospheric Arctic vortices. *J. Meteor. Soc. Japan,* **80,** 997–1012.

——, W. J. Randel, S. Pawson, P. A. Newman, and E. R. Nash, 1999: Persistence of the lower stratospheric polar vortices. *J. Geophys. Res.,* **104,** 27 191–27 201.

Wei, K., W. Chen, and R. H. Huang, 2007: Dynamical diagnosis of the breakup of the stratospheric polar vortex in the Northern Hemisphere. *Sci. China,* **50D,** 1369–1379.